# Complexity of quantum states in the two-dimensional pairing model

J. R. Armstrong
*Winona State University, 175 W. Mark St, PA 120, Winona, MN 55987, USA*

S. Åberg and S. M. Reimann
*Mathematical Physics, LTH, Lund University, Box 118, SE 22100 Lund, Sweden*

V. G. Zelevinsky
*NSCL and Department of Physics and Astronomy, Michigan State University, East Lansing, Michigan 48824, USA*

(Received 4 June 2012; published 5 December 2012)

It is known that many-fermion systems, such as complex atoms and nuclei, reveal (at some level of excitation energy) local signatures of quantum chaos similar to the predictions of random matrix theory. Here, we study the gradual development of such signatures in a model system of up to 16 fermions interacting through short-range pairing-type forces in a two-dimensional harmonic trap. We proceed from the simplest characteristics of the level spacing distribution to the complexity of eigenstates, strength, and correlation functions. For increasing pairing strength, at first, chaotic signatures gradually appear. However, when the pairing force dominates the Hamiltonian, we see a regression towards regularity. We introduce a "phase correlator" that allows us to distinguish the complexity of a quantum state that originates from its collective nature, from the complexity originating from quantum chaos.

DOI: 10.1103/PhysRevE.86.066204 PACS number(s): 05.45.Mt, 05.45.Gg

## I. INTRODUCTION

The harmonic oscillator potential confining a number of quantum particles has for many decades served as a paradigm to study many-body effects in finite quantum systems, ranging from atomic nuclei to quantum dots.

A new perspective has more recently opened up with ultracold bosonic or fermionic atoms in magneto-optical traps. The experimental possibilities to design the quantum confinement, together with tunable interactions between the atoms, nowadays allow unprecedented access to study the few- and many-body physics of complex quantum systems (see, for example, Ref. [1] for a review). While initially the focus was on Bose-Einstein condensation with millions of confined atoms, now also fermion confinement in the few-body limit has come into experimental reach [2]. A few theoretical works [3–6] (see also the recent review in Ref. [7]) have addressed this limit for an isolated harmonic trap, calculating ground-state energies, spectra, odd-even mass differences, and examined the role of angular momentum in two- and three-dimensional systems for various interactions.

The main aim of the present work is to examine the quantum properties of interacting fermions confined in a two-dimensional harmonic oscillator through the lens of quantum chaos. The fermions are assumed to interact through attractive and short-range pairing-type forces, analogously to what has been studied earlier in the context of nuclear physics [8–11]. At first, the nuclear theory was developed along lines similar to the BCS theory of superconductivity that is essentially exact only in the macroscopic limit (see Bohr, Mottelson, and Pines [8]). Methods to treat small numbers of particles were subsequently developed; see, for example, Refs. [12,13].

Short-ranged attractive forces account well for the effective interactions in the fermionic cold-atom systems mentioned above. Here, we examine how the complexity of the quantum states changes as the interaction strength is varied.

For particles in time-conjugate orbits, the overlap of the single-particle wave functions is maximum. For short-ranged interactions, we thus may expect the pairing model to describe the main physical observables well. Importantly, at comparable correlation strength, the pairing Hamiltonian allows one to extend the number of confined particles beyond what is possible for a direct numerical diagonalization of the full Hamiltonian.

The relationship between many-body physics and quantum chaos has been well studied in atomic [14] and nuclear physics [15–19], as well as in condensed-matter physics where it is sometimes formulated as a problem of many-body localization [20]. While a rigorous definition of quantum chaos in many-body systems remains elusive, it is an almost universal feature of interacting many-body systems that, at sufficiently large interaction strength, the eigenstates become exceedingly complicated superpositions of single-particle excitations with spectral statistics close to the random matrix limit [15,17–19,21–23]. We shall, however, see that the coherent structure of the pairing force may partly suppress such onset of complexity.

The standard signatures of chaos are usually recognized from the generic spectral statistics [21]. We also consider other measures of less pronounced, but perhaps not less significant, milestones on the road to chaos. It is a unique feature of the pairing force that it creates largely mixed states in the low-energy region. Even if gradual, there appear generic changes in the structure of individual many-body wave functions, strength functions, and related observables along the path to stronger interactions or higher excitations. These quantities probe the mixing of basis states and the systematically increasing complexity (determined through indicators such as informational entropies and inverse participation ratios), and the spreading widths of simple modes of excitations (determined through the strength function). For some of these quantities, one can compare our results with those for a random interaction, where

 

the matrix elements follow the Gaussian orthogonal ensemble (GOE). The latter is the appropriate ensemble for systems with time-reversal symmetry; see, e.g., Refs. [19,21]. We show that there are precursors of quantum chaos that are generated by the pairing interaction. For sufficiently large pairing strength, the chaotic properties are reduced, and we see the revival of regularity that is reflected in the spectral statistics.

## II. METHOD

In distinction to the BCS-type variational approaches, the pairing model used in the following is known as "exact pairing." It is described in detail in Refs. [12,13]. The method is briefly summarized below, adapted to the specific problem at hand.

The general Hamiltonian for $N$ fermions of mass $m$ confined by a two-dimensional harmonic trap (with oscillator frequency $\omega$) and interacting through a contact interaction is

$$H = \sum_{i}^{N}\left(-\frac{\hbar^2}{2m}\nabla_i^2 + \frac{1}{2}m\omega^2 r_i^2\right) + g'\sum_{i\neq j}\delta^{(2)}(\mathbf{r}_i - \mathbf{r}_j), \quad (1)$$

where the coupling constant $g'$ has a dimension of energy times area. The dimensionless coupling constant, $g$, is the ratio of the coupling strength $g'$ to the characteristic energy and squared length scale of the trapped system, $g = g'/(\hbar\omega\ell^2)$ and $\ell = (\hbar/m\omega)^{1/2}$. We consider the case of attractive interaction, $g < 0$. In this case, the Hamiltonian can be approximated by that of the pairing model,

$$H_p = \sum_{nm\sigma}\epsilon_n a^\dagger_{nm\sigma}a_{nm\sigma} + \frac{1}{4}g\sum_{nn'}G_{nn'}\sum_{mm'\sigma\sigma'}a^\dagger_{nm\sigma}\tilde{a}^\dagger_{nm\sigma}\tilde{a}_{n'm'\sigma'}a_{n'm'\sigma'}, \quad (2)$$

where $\epsilon_n$ are single-particle energies in the harmonic trap and the tilde indicates time reversal. The first term thus describes the (one-body) confinement part and the second term the (two-body) pairing interaction. The oscillator frequency, $\hbar\omega$, controls the strength of the one-body part, and the parameter $g$ controls the interaction part (the interaction matrix elements $G_{nn'}$ are defined below). We use here the (one-body) basis where each orbital $|nm\sigma\rangle$ is characterized by three quantum numbers, where $n$ is the main (radial) oscillator shell number (starting at 0), $m$ is the orbital angular momentum projection, and $\sigma$ is the spin projection. The time-reversal operation is defined as

$$\tilde{a}^\dagger_{nm\sigma} = (-1)^{n+1/2-m-\sigma}a^\dagger_{n-m-\sigma}. \quad (3)$$

The main quantum number, $n$, is not normally related to time-reversal symmetry; however, in this case it is equal to the maximum value of $m$ for a given shell. In two dimensions, $n$ and $|m|$ have the same parity so we can simplify the expression further,

$$\tilde{a}^\dagger_{nm\sigma} = (-1)^{1/2-\sigma}a^\dagger_{n-m-\sigma}. \quad (4)$$

The pairing matrix elements are calculated using the "quasispin" formalism applied separately to each $n$ shell. The pair creation and annihilation operators are represented as the "quasispin" generators of the SU(2) group,

$$L_n^- = \frac{1}{2}\sum_{m\sigma}(-1)^{1/2-\sigma}a_{n-m-\sigma}a_{nm\sigma},$$
$$L_n^+ = (L_n^-)^\dagger = \frac{1}{2}\sum_{m\sigma}(-1)^{1/2-\sigma}a^\dagger_{nm\sigma}a^\dagger_{n-m-\sigma}, \quad (5)$$

and the "$z$ component" of quasispin is

$$L_n^0 = \tfrac{1}{2}N_n - \tfrac{1}{4}\Omega_n, \quad (6)$$

where $N_n$ is the number of particles in the $n$th shell, and $\Omega_n$ is the degeneracy of this shell. The pairing Hamiltonian of Eq. (2) then can be rewritten as

$$H_p = \frac{1}{2}\sum_n\epsilon_n\Omega_n + 2\sum_n\epsilon_n L_n^0 + g\sum_{nn'}G_{nn'}L_n^+L_{n'}^-. \quad (7)$$

This Hamiltonian preserves the set of conserved partial quasispins $L_n$ or, equivalently, the partial "seniority" quantum numbers $v_n = 2(\Omega_n/4 - L_n)$ that measure the deviation of the quasispin $L_n$ from its maximum value $(\Omega_n/4)$ and essentially coincide with the number of unpaired particles in the $n$th shell. We shall often refer to the total seniority, or the total number of unpaired particles in the system, $v = \sum v_n$. If all pairing matrix elements are the same, $G_{nn'} = \text{const}$, the Hamiltonian $H_p$ has been shown to be integrable [24].

The conservation of seniorities allows us to write the matrix elements in a simple form in terms of the number of particles in a given oscillator shell, its degeneracy, and seniority. The diagonal matrix elements are

$$\langle\{N_n\},\{v_n\}|H_p|\{N_n\},\{v_n\}\rangle = \sum_n\left[\epsilon_n N_n + g\frac{G_{nn}}{4}(N_n - v_n)(\Omega_n - v_n - N_n + 2)\right], \quad (8)$$

where $|\{N_n\},\{v_n\}\rangle$ are many-body basis states. The unpaired particles do not interact in this model. However, they influence the dynamics indirectly by Pauli-blocking certain final states available for the pairs. The off-diagonal matrix elements correspond to the pair transfer, changing the occupancies of two orbits but keeping seniorities unchanged and the total particle number $N = \sum_n N_n$ fixed,

$$\langle\ldots,N_i+2,\ldots,N_{i'}-2,\ldots;\{v_n\}|H_p|\ldots,N_i,\ldots,N_{i'},\ldots;\{v_n\}\rangle = g\frac{G_{ii'}}{4}[(N_{i'} - v_{i'})(\Omega_{i'} - v_{i'} - N_{i'} + 2) \times (\Omega_i - v_i - N_i)(N_i - v_i + 2)]^{1/2}. \quad (9)$$

It remains to specify the interaction matrix elements denoted by $G_{ii'}$ in the above expressions. In Eq. (1), we indicated that we had used a contact interaction. The $\delta$-function potential has its problems in spatial dimensions larger than 1. This problem is well known in the literature; see, for example, Refs. [25–29]. A remedy often is a cutoff that effectively renormalizes the interaction strength (as extensively discussed in Ref. [30]). Here we followed this approach and performed the calculations in a model space of $n_{\max} = 6$ oscillator shells for particle numbers up to $N = 9$, as was done in

Ref. [6], where the pairing calculation was compared to exact diagonalization of the full Hamiltonian, $H$. For systems with up to $N = 16$, we include $n_{\max} = 9$ oscillator shells. Regarding the interaction, the theory requires a degenerate multiplet for the pairs, which is broken by the $\delta$ function form of the two-body interaction. Thus, we must average the interaction within a given oscillator shell. In the actual calculations, the interaction parameters, $G_{ii'}$, are equal to

$$G_{ii'} = \frac{1}{\sqrt{\Omega_i \Omega_{i'}}} \sum_{mm'} \langle i'm', i' - m' | \delta^{(2)}(\mathbf{r} - \mathbf{r}') | im, i - m \rangle. \tag{10}$$

The Schrödinger equation for the pairing Hamiltonian,

$$H_p |\alpha\rangle = E_\alpha |\alpha\rangle, \tag{11}$$

is finally solved by numerical diagonalization of submatrices corresponding to the good quantum numbers discussed above.

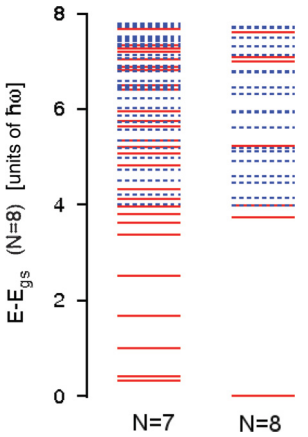


FIG. 1. (Color online) Spectra of low-lying states for seven and eight particles for $g = -5$. The red solid lines are the lowest-seniority states, $v = 0$ for eight particles and $v = 1$ for seven particles. The dotted blue lines are the states with one broken pair, which clearly show the pairing gap. The energies (in units of $\hbar\omega$) are measured relative to the ground state of the eight-particle system.

## III. RESULTS

The Hamiltonian, Eq. (2), was diagonalized for particle numbers $N$ from $N = 2$ to $N = 16$. The energy spectra for $N < 9$ were reported in Refs. [6,31], where the pairing results for low-lying states were compared with results from exact diagonalization performed on the same Hamiltonian, Eq. (1), with sums over all two-body pairs rather than just those in time-reversed orbits, Eq. (2). Here, we discuss the complexity of eigenstates in the full model space when the effective interaction strength $g$ grows in magnitude from the smallest values near zero, to $g = -10$, where the pairing interaction dominates.

An example of the spectrum for a system with $N = 7$ and $N = 8$ at $g = -5$ is shown in Fig. 1. The difference between even- and odd-numbered systems is clear, with the gaps between the different seniorities being indicative of the size of the pairing effect.

In Fig. 2 the lowest-seniority $v = 0$ energy levels are shown for a system of 16 particles for different interaction strengths. For the lowest strengths, the confinement potential dominates and typical jumps of $2\hbar\omega$ can be seen, corresponding to pair excitations from one oscillator shell to another. This oscillatory behavior is more or less smeared out when $g = -3$. With even larger interaction strength, the spectrum becomes more and more dominated by the pairing part. In all cases, the density of (all) states for a given seniority has a generic Gaussian shape [21], as was found originally in the two-body random ensemble [32], in contrast to the semicircle shape in the full Gaussian orthogonal ensemble, explained in detail in Ref. [21] and confirmed in large-scale nuclear shell-model diagonalization [15].

The off-diagonal interaction broadens the distribution but does not change it qualitatively: Figure 3 shows the density of $v = 0$ states for a system of 16 particles in nine oscillator shells. In this case, there are 8095 states with this good quantum number. Naturally, only the lower part of the spectrum is physically relevant. But, as is often done when quantum complexity is investigated [15,19], the whole set of eigenstates in the restricted model space is considered in the analysis. Notice that $v = 0$ requires $v_n = 0$ for all $n$. The lowest $v = 0$ state corresponds to the total ground state of the system, and the excited states are constructed by redistribution of unbroken fermion pairs. States where these excitations are coherent or collective are usually called pairing vibrations [11,33], which we shall come back to later. The pairing interaction consistently pushes the states to lower energies (Fig. 3). Lower-lying states thus are expected to be considerably more "mixed" than states in the upper end of the spectrum. This differs from how a "generic" (or random) interaction mixes the states, shifting energies to lower and higher energies in a symmetric fashion.

In the following, in Sec. III A we investigate the signatures of chaos in terms of spectral statistics. The complexity and

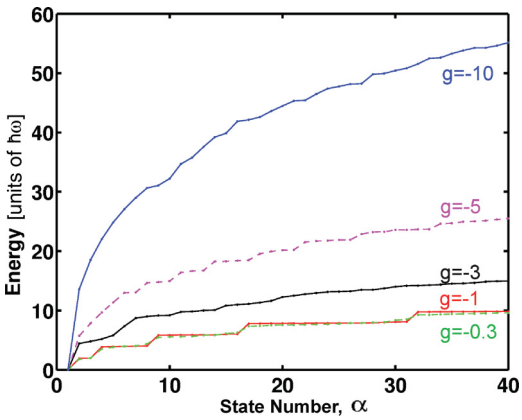


FIG. 2. (Color online) Energies relative to the ground state (in units of $\hbar\omega$) of the 40 lowest $v = 0$ states for the 16-particle system. The curves correspond to the pairing interaction strength $g = -0.3, -1, -3, -5$, and $-10$ (from below).

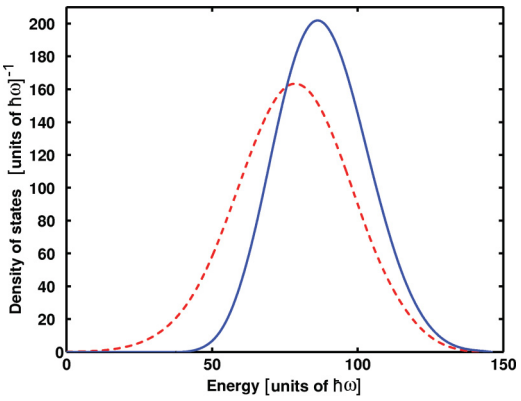


FIG. 3. (Color online) Density of seniority zero states as a function of energy for a system of 16 particles interacting with the pairing interaction strength $g = -0.3$ (solid line) and $g = -5$ (dashed line). In each case, 8095 states are included, corresponding to $n_{\max} = 9$ oscillator shells.

localization of the eigenstates are studied in Sec. III B. Strength functions and their relation to the average interaction strength are studied in Secs. III C and III D introduces a tool to investigate phase correlations between the components of a wave function.

### A. Spectral statistics

The simplest measure of quantum chaos is usually the *nearest-neighbor spacing distribution* (NNSD), $P(s)$, where $s = (E_{\alpha+1} - E_\alpha)/D_n^{(\alpha)}$ is the energy distance to the nearest neighbor in the units of the local mean distance, $D_n^{(\alpha)}$. Each state in the considered energy spectrum has the same set of good quantum numbers, $\{v_n\}$. For states of different symmetry properties, or in weakly interacting systems with many degeneracies, levels can come arbitrarily close to one another, resulting in a Poisson distribution of level spacings. In the case of stronger interactions, the levels of the same symmetry repel each other, and $P(s)$ generically evolves to the Wigner distribution, which is very close to what is obtained in the GOE. The conjecture [34] that relates signatures of quantum chaos (through spectral statistics, e.g., NNSD) to classical chaos is valid for one-body systems. We apply it here for the many-body system, and, following the usual terminology, we phrase GOE properties in the many-body system as "quantum chaos."

The mean level spacing was defined as $D_n^{(\alpha)} = (E_{\alpha+n} - E_{\alpha-n})/(2n)$, where we used $n = 2,3,5$, which did not cause dramatic changes to $P(s)$. For the strongly interacting cases, the changes were very small. At weaker interaction, the larger values of $n$ would push the high-lying fluctuations to even higher values of $s$ and increase the magnitude of the peak at $s = 0$, but otherwise had little effect. In order to avoid edge effects of the considered spectrum, only the central 50% of the states are included in the analysis. The NNSD distributions are commonly fit with the Brody parametrization [35],

$$P(s) = (1+\alpha)s^\alpha \exp(-Ks^{1+\alpha}),$$
$$K = [\Gamma((2+\alpha)/(1+\alpha))]^{1+\alpha}, \quad (12)$$

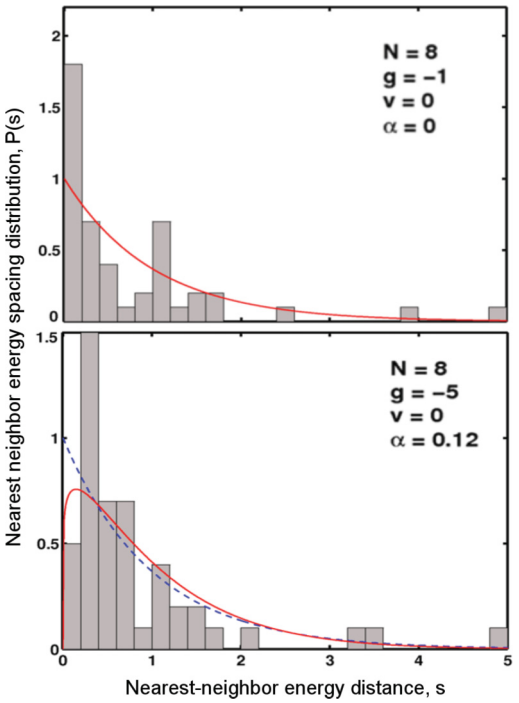


FIG. 4. (Color online) Nearest-neighbor spacing distribution for eight particles, with Brody fit (solid line). (Upper panel) $g = -1.0$ and $v = 0$. $D_n^{(\alpha)}$ is calculated with $n = 3$. The bin width is 0.2 units of $s$. The Brody parameter extracted from the fit is $\alpha = 0$. (Lower panel) $g = -5.0$ and $v = 0$. The extracted Brody parameter is $\alpha = 0.20$. The dashed line shows the Poisson limit that coincides with the Brody fit for the case $g = -1$.

where $\alpha$ is the single fit parameter that is also called the Brody parameter. A value $\alpha = 0$ corresponds to the Poisson case (regular), and $\alpha = 1$ corresponds to the Wigner case (chaos). The value of $\alpha$ thus can give a rough hint about the character of the spectrum in the regions between regularity and chaos.

Upper and lower parts of Fig. 4 show $P(s)$ for eight particles with $v = 0$ in the cases of weak and strong interaction, respectively. Only 49 levels, constituting the central 50% of the spectra, are considered. This limits the accuracy of the analysis. For weak interactions, we see indications of a Poisson distribution ($\alpha = 0$).

For the strongly interacting case, the distribution maximum moves to a higher value of $s$. It is not a Wigner distribution but it indicates a situation between regularity and chaos, and the Brody analysis gives $\alpha = 0.20$. Similar results (with more levels and, thus, better statistics) are obtained for $v = 2$ states not shown here.

Compared to the eight-particle system, the analysis of the spectrum properties for the 16-particle model system is more accurate as the statistics is improved significantly due to the considerably larger energy stretch of 4050 levels for $v = 0$ (central part of the spectrum). In Fig. 5 we show the NNSD for 16 interacting particles with pairing strengths $g = -0.3, -1, -3$, and $-10$. The complexity of the spectrum gradually increases, with a completely regular spectrum for the weakest interaction and then reaching a maximal degree of chaos for $g = -3$ (or slightly above) with $\alpha = 0.29$. The complexity of the spectrum then *decreases* as the pairing

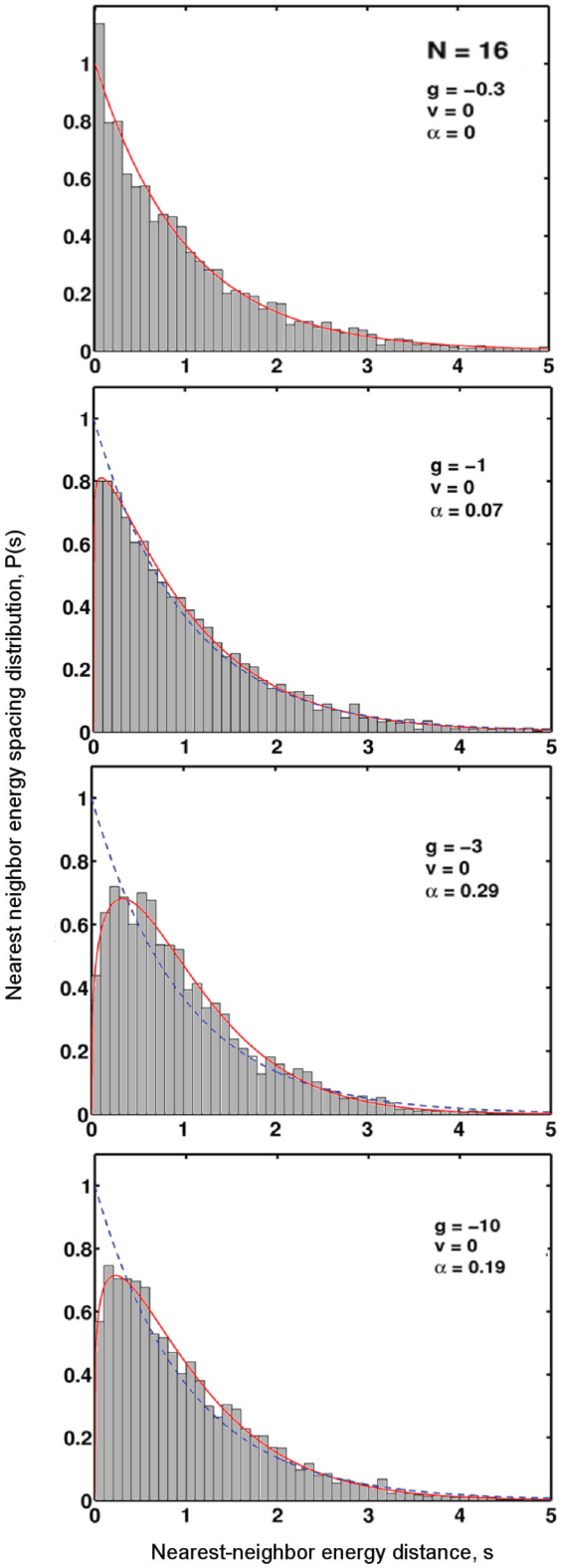


FIG. 5. (Color online) Nearest-neighbor spacing distributions for 16 particles and seniority $v = 0$, for different interaction strengths $g$. The Brody fit is shown by a red solid line, and the Poisson limit is shown by a dashed line. The bin width is $0.1s$ and $D_n^{(\alpha)}$ is calculated with $n = 5$. From top to bottom, for $g = -0.3$, the Brody parameter fit gives $\alpha = 0$; for $g = -1$, $\alpha = 0.07$; for $g = -3$, $\alpha = 0.29$; and for $g = -10$, the Brody fit gives $\alpha = 0.19$.

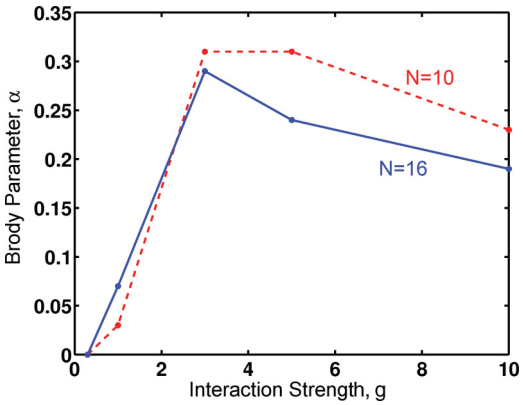


FIG. 6. (Color online) Brody mixing parameter versus pairing strength for systems with 16 (solid line) and 10 particles (dashed line).

strength is growing further, and, at the very large strength, $g = -10$, the Brody parameter falls to $\alpha = 0.19$. In Fig. 6 the fitted Brody parameter is shown as a function of pairing strength for systems with 16 and 10 particles revealing the common pattern. The general trend seen in Fig. 5 was found to be quite robust, with respect to changes in the model space size, changes in $D_n^{(\alpha)}$, and changes in the selection of energy states. For example, very similar results are obtained if the lowest 10% of the states (excluding the two lowest states) are used in the analysis instead of the central 50%.

The observed behavior of the complexity of the system with increasing pairing strength, regular to chaos (or rather mixed) and back to regular, may be understood in the following way. At small strength, the Hamiltonian is dominated by the (regular) harmonic oscillator part, and at very large strength it is dominated by the pure pairing Hamiltonian. For moderate interaction strengths, the effects of the two parts of the Hamiltonian are of similar size, and the mixing causes the irregular behavior. The transition from the harmonic oscillator to the pairing dominance was also seen from the analysis of the energy spectra in Fig. 2.

### B. Complexity and localization of the eigenstates

The eigenstates $|\alpha\rangle$ are written as a linear combination in the many-body basis set $|k\rangle \equiv |\{N_n\}\{v_n\}\rangle$ of noninteracting particles,

$$|\alpha\rangle = \sum_k^{\mathcal{N}} C_k^{(\alpha)} |k\rangle, \tag{13}$$

where $\mathcal{N}$ is the number of basis states. The statistical properties of the amplitudes $C_k^{(\alpha)}$ reflect the degree of correlation in the specific eigenstate $|\alpha\rangle$ with respect to the chosen basis. The complexity (or, in other words, the mixing of the basis states) is caused by the two-body interaction. A convenient characteristic measure for quantum-chaotic behavior is given by the *informational*, or *Shannon, entropy* calculated for each individual eigenstate $|\alpha\rangle$,

$$S^{(\alpha)} = -\sum_k^{\mathcal{N}} \left|C_k^{(\alpha)}\right|^2 \ln \left|C_k^{(\alpha)}\right|^2. \tag{14}$$

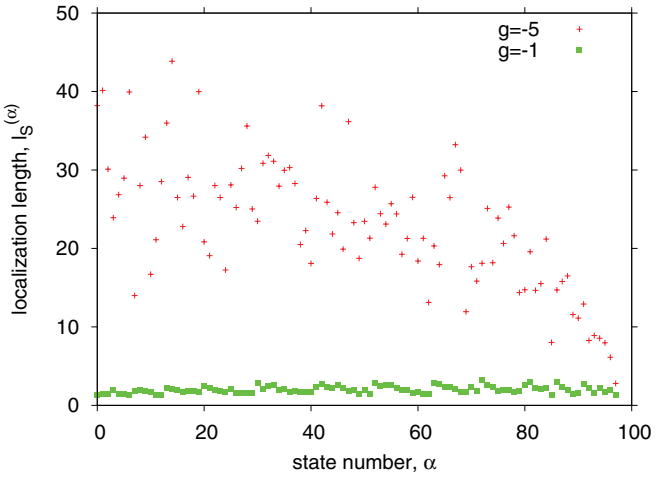


FIG. 7. (Color online) Informational entropies calculated for eight particles; states with $v = 0$ and $g = -1$ (green points) and interaction strength $g = -5$ (red crosses). The exponent of the entropy (localization length) is plotted against the eigenstate number, where the eigenstates are placed in order of increasing energy. There are 98 $v = 0$ states giving $l_S^{\mathrm{GOE}} = 47$.

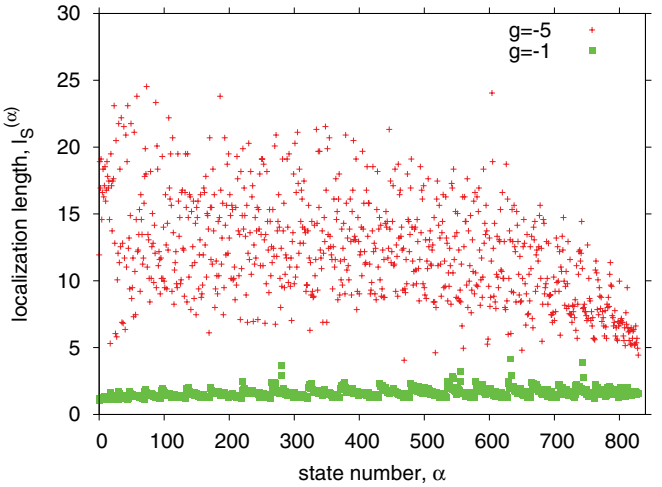


FIG. 8. (Color online) Same as described in the caption to Fig. 7 but with $v = 2$. There are 829 $v = 2$ states.

This quantity is basis dependent, revealing the relative complexity of the states $|\alpha\rangle$ with respect to the basis states. In the eigenbasis, it vanishes, and in a completely mixed, "*microcanonical*" state, when $|C_k^{(\alpha)}| = 1/\sqrt{\mathcal{N}}$ for all $\alpha$, it takes the maximum value of $\ln \mathcal{N}$. We have to note that this entropy is insensitive to the relative phases of the components of the wave functions and, therefore, cannot distinguish between chaotic mixing and coherent collectivization, a collective mode that has coherent contributions from many states.

The exponent of the entropy, that corresponds to a "*localization length*" in Hilbert space,

$$l_S^{(\alpha)} = \exp S^{(\alpha)}, \tag{15}$$

is a measure of the number of significant basis components contained in the eigenstate $|\alpha\rangle$. The mean value of such a length in the random matrix limit of the GOE is $l_S^{\mathrm{GOE}} \approx 0.48\mathcal{N}$ [15,36]. Deviations from this limit indicate the incomplete mixing of the basis states.

Figures 7 and 8 show the localization length of individual eigenstates calculated for eight particles, $g = -1$ and $g = -5$, and seniority values $v = 0$ and $v = 2$, respectively. There are typically a few low-lying states with a large amount of mixing, usually of collective (vibrational) nature. The single pairing vibration mode with the same quantum numbers as the ground state is expected above the pairing gap. This is observed in the case of $g = -5.0$, where we find 98 states with seniority $v = 0$: the presence of low-lying, highly mixed states (including a few that approach the GOE limit of $l_S^{\mathrm{GOE}} \approx 47$). Other $v = 0$ states are noncollective (energetically nonfavorable redistribution of the pairs over the levels).

For seniority $v = 2$ states there are fewer pairs, but there are more ways to arrange the particles. Due to the special nature of the pairing interaction, there exist separate "families" lying in the spectrum. For $v = 2$, there are several configurations that do not mix with each other by a pure pairing interaction, for example, in terms of partial seniorities, $|\{v_n\}\rangle = |1,1,0,0,0,0\rangle, |0,2,0,0,0,0\rangle, |1,0,1,0,0,0\rangle$, and so on. Each of these configurations gives rise to their own separate family visible at weak interaction. They are seen as the 20 vertical sequences of states in Fig. 8 for the case of $g = -1$. These distributions become overlapping at stronger interaction. The entropies are considerably lower for the higher-seniority states: they have a smaller number of basis states, since pair transfers are strongly blocked. In the case of weaker interactions, there is much less mixing, which noticeably occurs mainly in the higher-seniority states.

Figure 9 shows the localization length of individual seniority $v = 0$ eigenstates calculated for 16 particles with $g = -5$. There are 8095 basis states, implying a GOE limit, $l_S^{\mathrm{GOE}} \approx 3847$. Several low-lying states are strongly mixed, as seen from the large localization length approaching the GOE limit. It is striking how the low-energy states consistently have the largest amount of mixing. That the pairing interaction has

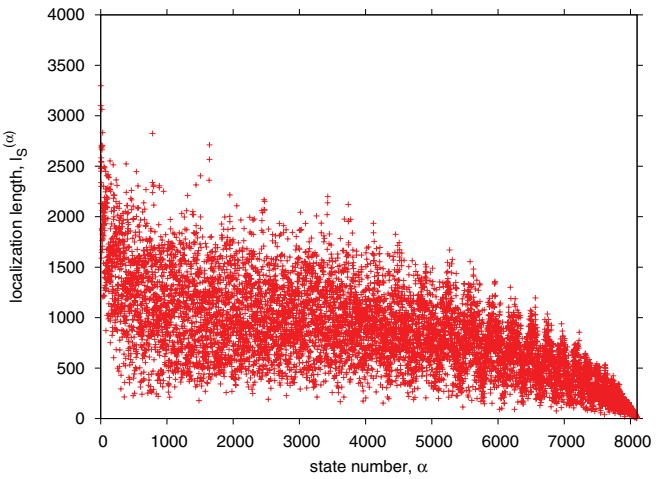


FIG. 9. (Color online) Same as in Fig. 8 but for 16 particles with $g = -5.0$ and seniority $v = 0$. The calculation is performed with $n_{\max} = 9$ oscillator shells, giving 8095 $v = 0$ states, implying the GOE limit $l_S^{\mathrm{GOE}} = 3847$.

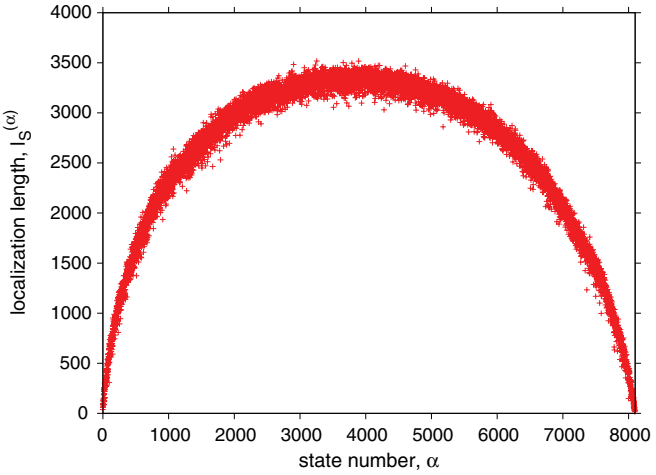


FIG. 10. (Color online) Same as in Fig. 9 but nondiagonal matrix elements of the Hamiltonian have been given random signs.

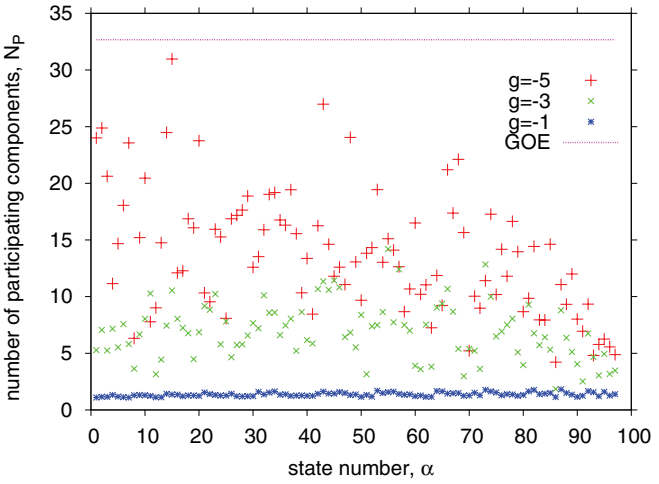


FIG. 11. (Color online) Number of principal components ($N_P$) calculated for eight particles with $g = -1.0, -3.0, -5.0$, and $v = 0$. The $N_P$ is plotted against the eigenstate number, where the eigenstates have been placed in order of increasing energy. The dotted line represents the GOE limit of 32.67.

the strongest effect on the energy of low-lying states was also seen in Fig. 3.

The localization length of individual eigenstates in the case of the pairing interaction largely deviates from the more general picture of other types of interactions, as, e.g., the corresponding results from a nuclear shell-model calculation in Ref. [22]. The Shannon entropy then shows a broad, inverted U shape, with the maximum in the middle of the spectrum. The entropy in average is diminished towards the ends, revealing the weaker mixing because of the lower level density. The decrease at higher energies trivially appears due to the truncated model space.

The special nature of the pairing interaction implies strong coherence of nondiagonal matrix elements reflected in largely the same sign of the matrix elements. If these non-diagonal matrix elements are given random signs while the size of the matrix elements is kept unchanged, the coherent nature of the Hamiltonian is lost, and the Shannon entropy indeed shows the "generic" U-shaped behavior; see Fig. 10.

It is interesting to note that also the *fluctuations* of the information entropy are considerably larger than what is obtained with a generic Hamiltonian, such as the random-sign case discussed above or the nuclear shell model [22], where neighboring states show a similar amount of mixing. The pairing Hamiltonian implies strongly nonergodic wave functions. In Fig. 9 we note extreme cases where one state has a localization length $l_S \approx 200$ and a close-lying state has $l_S \approx 2800$.

For an odd-numbered particle system (not shown here) the results are similar, the main difference being the much greater number of states in the odd system (e.g., for seven particles there are 2479 total seniority $v = 1$ and seniority $v = 3$ states, whereas for eight particles there are 948 total seniority $v = 0$ and $v = 2$ states). Also, the low-seniority distribution now is more complicated since it contains multiple seniority distributions over the shells. This differs for systems with an even particle number where seniority $v = 0$ has only one configuration with all partial seniorities equal to zero.

Another quantity related to the complexity of an eigenstate is the number of principal components ($N_P$), or the *inverse participation ratio*, defined as

$$N_P^{(\alpha)} = \left[ \sum_k^{\mathcal{N}} \left| C_k^{(\alpha)} \right|^4 \right]^{-1} . \tag{16}$$

The average over the GOE limit here is $\mathcal{N}/3$, that is, 32 in the case of $v = 0$ states for eight particles.

The complexity of wave functions at different excitation energies measured by the $N_P$ is similar to what is seen from the information entropy. The numerical results for eight particles are shown in Fig. 11 as a function of eigenstate number, $\alpha$. One state approaches the GOE value, while the others strongly fluctuate (for the strongest interaction with $g = -5$), until the very end of the spectrum, where the $N_P$ diminishes as in the case of the entropy. The $g = -3$ case seems to be similar to the entropy calculations: a highly mixed state followed by states with fewer components until some minimum in a number of components is reached, and then the cycle repeats. In the case of the weakest interaction (with $g = -1$), on average, the states contain between one or two components, so any further structure is lost on this scale; still, with a closer look, one can see a pattern similar to what is seen for $g = -3$.

In models with more rich interactions, the two measures of complexity, information entropy and $N_P$, are essentially equivalent and are smooth functions of the excitation energy. They relate to the thermodynamic variables in the understanding of the thermalization process due to chaos, cf. Sec. IV B. We shall see that for the pairing interaction the two measures differ. The information entropy is especially sensitive to small components due to the logarithm, and there are many fluctuations still in this low-dimension regime.

By constructing the ratio

$$r^{(\alpha)} = l_S^{(\alpha)} / N_P^{(\alpha)}, \tag{17}$$

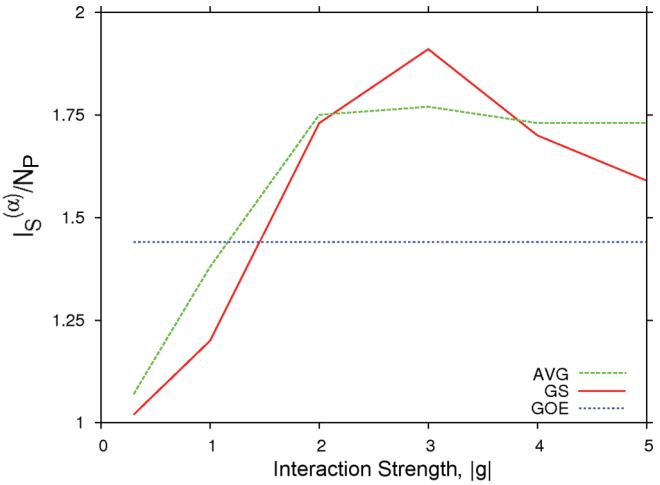


FIG. 12. (Color online) The ratio of the exponent of the entropy and the $N_P$, $r^{(\alpha)}$, calculated for eight particles as a function of $|g|$. We plot the average ratio for all $v = 0$ states (AVG, dashed line) and the ratio for the ground state (GS). The dotted line represents the GOE limit of 1.44.

the dependence on the dimension $\mathcal{N}$ is eliminated, and we get $r^{(\alpha)} = (0.48\mathcal{N})/(\mathcal{N}/3) \approx 1.44$ in the GOE limit. In Fig. 12 we show $r^{(\alpha)}$ for eight particles as a function of interaction strength, comparing the ground-state value to the value averaged over all states. Both $r^{(\alpha)}$ values cross the GOE limit at smaller values of $|g|$. This is readily understood because, in the noninteracting limit, the ratio $r^{(\alpha)}$ is equal to 1 ($I_S^{(\alpha)} = N_P = 1$). We see that the ground-state ratios are slower than the average to come above the GOE line, but eventually they surpass the average ratio. They finally fall below the average ratio again at larger values of $|g|$ (but are still above the GOE limit). As mentioned above, the entropy $I_S^{(\alpha)}$ is more sensitive to the fluctuations, especially for the highly mixed ground state, which allows the ground state to overtake the average ratio at the interaction strength, where strong mixing begins. As expected, in a system with eight particles the $N_P$ increases as a function of $|g|$, from 1.37 to 6.93 to 13.74 for $g = -1, -3$, and $-5$. The average value of $r^{(\alpha)}$, however, does not quite follow that trend, changing from 1.45 for $g = -1$ to 1.77 for $g = -3$, while then falling slightly to 1.73 for $g = -5$.

### C. Strength function

The strength function, often called the "local density of states,"

$$F_k(E) = \sum_\alpha \left|C_k^{(\alpha)}\right|^2 \delta[E - (E_\alpha - E_k)], \qquad (18)$$

shows how a given basis state $|k\rangle$ is spread over the eigenstates $|\alpha\rangle$ of the system along the energy scale. By subtracting the energy of the basis state, $E_k$, from the eigenenergies, $E_\alpha$, the strength function $F_k$ becomes centered around $E = 0$ for each $k$.

One can look at the strength function of an individual basis state, $F_k(E)$, or make an average of several functions in order to get an average strength function averaged over all $\mathcal{N}$ states. Since the maximum of each individual strength function, $F_k(E)$, is centered around the energy of the basis state, $E_k$, the averaged strength function, $\bar{F}$, is centered around $E = 0$.

Strength functions and their evolution as a function of the interaction between the particles, from quadratic ("golden rule") to linear dependence on the interaction strength, are discussed in great detail in Refs. [15,37–39]. In the noninteracting system the strength function, $F_k$, is concentrated at $E = 0$. As the interaction is increased, the strength of the state gets fragmented among surrounding eigenstates. At this stage, the strength is typically described [17] by a Breit-Wigner shape with a width, $\Gamma$, related to the squared average off-diagonal matrix element,

$$\Gamma_{\rm GR} = 2\pi\rho(E)\langle V^2\rangle, \qquad (19)$$

where $\rho(E)$ is the mean density of states connected to a given state by the interaction matrix elements $V$. This "golden rule" (GR) result is valid until $\Gamma$ spreads to the regions with significantly different level density or/and coupling matrix elements.

The average strength function for $N = 8$ with interaction strengths $g = -1, -3$, and $-5$ is shown in Fig. 13. For the weak interaction, $g = -1$ case, the central peak is very narrow, and there is very little fragmentation of the strength function. When the interaction is increased to $g = -3$, we see a broadening of the central peak and slight left-right asymmetry that becomes more pronounced for $g = -5$, where the peak is noticeably displaced to the right of zero. Including more states when building the average strength function changes the result only slightly. The value for the spreading width, $\Gamma_s$, is extracted from the cumulative strength function made by adding all individual strength functions with no averaging and displayed in Table I along with the "golden rule" widths, $\Gamma_{\rm GR}$, calculated after Eq. (19). Due to the sharpness of the peak in the case of the weakest interaction, its width is essentially uncertain. For the largest strengths the golden rule prediction

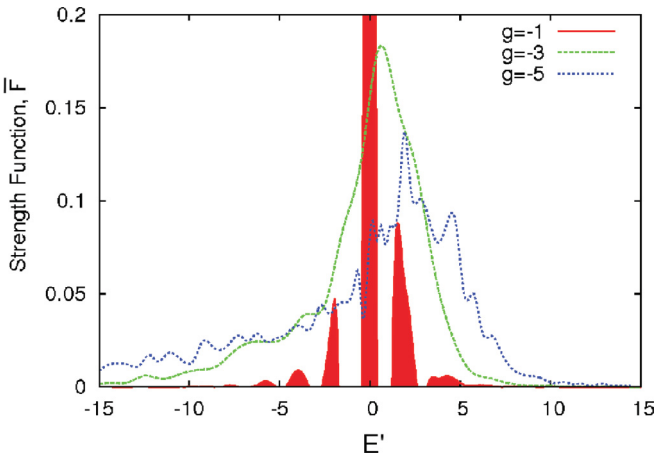


FIG. 13. (Color online) Strength function, $\bar{F}$, for seniority $v = 0$ states of eight particles with interaction strengths, $g = -1$, $g = -3$, and $g = -5$. The maximum of $\bar{F}$ reaches 0.65 (outside the scale in the figure) in the $g = -1$ case. The strength is plotted with respect to the energy difference of the eigenstate and the energy centroid of the basis state before diagonalization. The energy is expressed in units of $\hbar\omega$.

TABLE I. Table of calculated widths, $\Gamma_{GR}$ [Eq. (19)], and widths extracted from strength functions, $\Gamma_s$. Each row is for a certain system, specified by the particle number and $g$ value.

| N | \|g\| | $\Gamma_s$ | $\Gamma_{GR}$ |
|---|---|---|---|
| 6 | 1 | 0.12 | 0.24 |
| 6 | 3 | 2.31 | 2.24 |
| 6 | 5 | 4.66 | 6.54 |
| 8 | 1 | 0.14 | 0.29 |
| 8 | 3 | 3.31 | 2.69 |
| 8 | 5 | 5.98 | 7.79 |

overestimates the widths by about a factor of 1.3. That is, the strength function is still not as wide as predicted by the standard theory with significantly fragmented strengths.

The origin of the left-right asymmetry in the tails could be that the eigenstates that make up the lower part of the spectrum often have many significant components (see Fig. 3), thus amplifying the strength going to large negative values of $E$. The shift of the peak to the right, $E > 0$, occurs if a basis $k$ state has most of its strength in an eigenstate that is somewhat higher in energy (by about 2–3 $\hbar\omega$). We believe that this effect originates from the truncation. (For eight particles we have used $g = -5$ in a model space of six harmonic oscillator shells.)

### D. Phase correlator

The degree of mixing of states in the low-energy region was characterized in terms of the information entropy or the $N_P$, as discussed in Sec. III A. Some of the highly mixed states may carry a large amount of coherence or collectivity, while other states are mixed incoherently. To identify collective states among highly mixed states, we introduce the *phase correlator* of a given eigenstate,

$$P^{(\alpha)} = \frac{1}{\mathcal{N}} \sum_{kk'}^{\mathcal{N}} C_k^{(\alpha)} C_{k'}^{(\alpha)*}. \tag{20}$$

i.e., we take the average of all matrix elements of the density matrix for a given eigenstate $\alpha$. If there are no correlations between the signs of the wave function components, only diagonal terms contribute, giving $P^{(\alpha)} \sim 1/\mathcal{N}$. Collective states are usually characterized by strong correlations between the signs of components corresponding to basis functions (obviously, the discussion of collectivity as well as chaoticity only makes sense with respect to a certain basis set). Such correlations are recorded by the phase correlator, giving values larger than $1/\mathcal{N}$. For a unique correlated state where all the amplitudes are equal and of the same sign, the extreme limit of the phase correlator is $P^{(\alpha)} = 1$. Values close to one point towards a collective superposition of the basis states, such as the paired ground state. By construction, the phase correlator is always positive. Since the average over all eigenstates value of the phase correlator is

$$\langle P^{(\alpha)} \rangle = 1/\mathcal{N}, \tag{21}$$

the sum over all eigenstates always fulfills

$$\sum_{\alpha}^{\mathcal{N}} P^{(\alpha)} = 1. \tag{22}$$

This is a *sum rule* for the phase correlators; if one unique correlated state with index $\alpha$ picks all correlation [$P^{(\alpha)} = 1$], all other states $\alpha' \neq \alpha$ must have $P^{(\alpha')} = 0$.

In the GOE limit, the spreading (standard deviation) of the phase correlator becomes

$$\sigma_P^{\mathrm{GOE}} = \sqrt{\langle (P^{(\alpha)})^2 \rangle - \langle P^{(\alpha)} \rangle^2} = \frac{\sqrt{2}}{\mathcal{N}}. \tag{23}$$

For eigenstates of the pairing Hamiltonian, $\sigma_P$ becomes considerably larger. For example, for the seniority zero states in the system of 16 particles with $g = -5$, we find $\sigma_P = 36.6\,\sigma_P^{\mathrm{GOE}}$. The phase correlator of individual states, and the distribution of the phase correlator, provides important information about the system. Although the information entropy may approach the GOE limit, the phase correlator may show large deviations from this limit, indicating coherent, collective mixtures rather than incoherent, chaotic wave functions.

In Fig. 14 we plot the phase correlator of the states $|\alpha\rangle$ against their energy $E_\alpha$ for eight particles and $g = -5.0$. Two states have phase correlators separated from the rest with considerably larger values. These states are the ground state and the first excited state. The ground state is strongly coherent with $P = 0.57$, which is far higher than for any other state. The first excited state is a pairing vibrational excitation, with $P = 0.15$. For the 16-particle system with the same interaction strength, the situation looks similar (see Fig. 15) with the ground state picking up the dominant part of the phase correlator, with a value very close to the one above. Seven excited states have $P$'s larger than 0.03. The remaining 8087 states share the remaining $P$ of 0.2, where about half the states have $P$'s smaller than $10^{-7}$. This is considerably smaller than the GOE value ($\approx 10^{-4}$), again emphasizing the

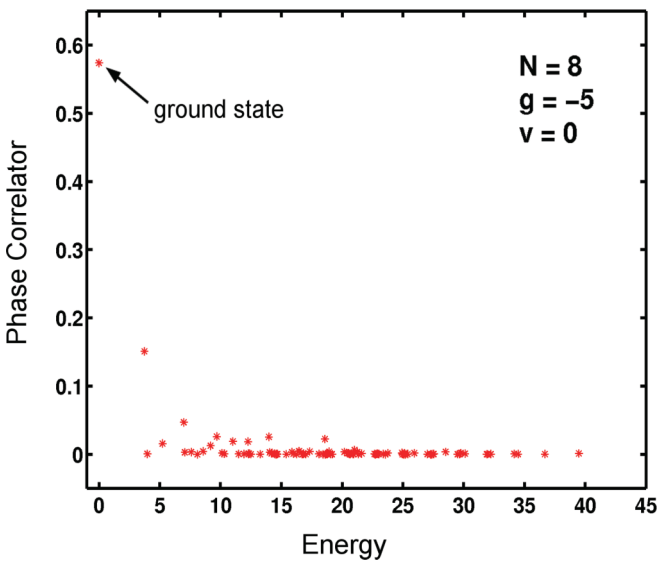


FIG. 14. (Color online) The phase correlator vs the eigenenergies. This plot is for eight particles, $g = -5.0$, and $v = 0$. All 98 states are shown.

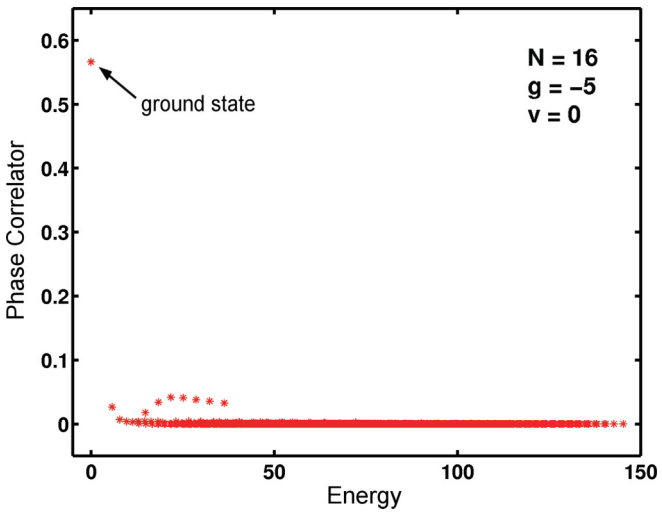


FIG. 15. (Color online) Same as in Fig. 14 but for 16 particles. All 8095 states are shown.

very different nature of the pairing force as compared to a generic force.

The phase correlation statistics thus differs markedly for the pairing Hamiltonian as compared to the GOE case.

## IV. DISCUSSION: CHAOS, THERMALIZATION, AND SPECIFICS OF PAIRING INTERACTION

### A. Onset of chaos

The coherent nature of the ground state and some manifestations of chaotic properties at higher excitation energy are properties of pairing Hamiltonians already mentioned in the literature [13,40,41]. These features seem to make the ground state and the first excited pair-vibrational state(s) of a much different character than the remainder of the spectrum, cf. Figs. 14 and 15. Chaotic features were found only at intermediate interaction strength, between the limits of weakly interacting particles and of strong pairing.

Estimates for the appearance of chaos in many-body systems can be made, based on quite general considerations. According to Ref. [42], the condition for onset of many-body chaos based on the average interaction strength and level spacing is given by

$$V \gg \frac{1}{\pi^2}\sqrt{d_f/\rho(E)}, \tag{24}$$

where $\rho(E) = 1/D$ is the global average level density used above, $D$ is the average spacing between two neighboring states, and $d_f$ is the average energy spacing between two states that are directly coupled by the interaction. When $g = -5$, $V$ is of order unity, and the right-hand side of Eq. (24) is about 0.05. Even for $g = -1$, $V$ is greater by a factor of 4. However, the authors of Ref. [42] comment that this condition is not always strong enough and that, since $d_f$ is usually much larger than $D$, a stronger definition would be $V > d_f$.

Indeed, in Refs. [17,43], the onset of many-body chaos was found to take place when

$$V \gtrsim 0.5 d_f. \tag{25}$$

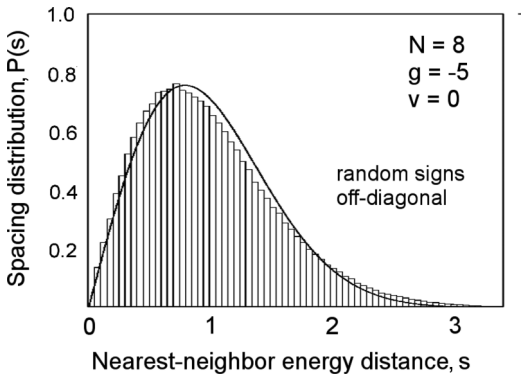


FIG. 16. NND for the eight-particle system ($v = 0, g = -5$) with random signs for nondiagonal matrix elements. The full curve is the Wigner limit of full chaos.

In our case, for 8 particles, $V = 1.12$ and $d_f = 1.08$, and, for 6 particles, $V = 1.03$ and $d_f = 1.26$. According to the second condition, at this strength of the interaction ($g = -5$), we are just on the edge of chaotic behavior. For 16 particles we find that $V$ is clearly larger than $d_f$ when $-g > 3$; e.g., for interaction strength $g = -5$ we have $V = 1.91$ and $d_f = 0.74$, and we thus would expect the system to show chaotic features.

However, these estimates for the onset of chaos refer to generic Hamiltonians. The pairing Hamiltonian is special containing large amounts of correlations. In the matrix representation this is seen as large coherence in the signs of nondiagonal matrix elements. We found that the complexity of the eight-particle system ($v = 0$ states) with $g = -5$ was not so large ($\alpha = 0.20$) as could be expected from the relations above. However, if we modify the Hamiltonian matrix in such a way that all matrix elements are fixed, but the signs of the nondiagonal matrix elements are made random, the above estimates become the same. Indeed, this implies that the system becomes almost fully chaotic; see Fig. 16.

### B. Thermalization

From a viewpoint of the reaction of a system to external perturbations, it is important to understand the statistical distribution of interacting particles over the orbitals in the confining potential. The evolution of the shell occupancies as the interaction is increased is seen in Fig. 17 (for 6 particles representing a closed shell). For $g = -1.0$, we still have a sharp Fermi level, with almost no occupancy leaking out to the higher shells. The leakage increases with interaction strength, until $g = -5$, the Fermi surface is smeared out, and the occupancies decrease exponentially with the oscillator shell number, as is seen explicitly for the examples with 8 and 16 particles (at $g = -5$) in Fig. 18.

This is to be expected as the increased interaction amplifies the mixing and involves basis states with particles in the higher shells. As it was repeatedly argued; see, for example, Refs. [14,15,22,44], chaotic mixing by generic internal interactions is essentially equivalent to thermalization by the contact to a heat bath. The incoherent interactions in a many-body system may play the role of a thermostat. It is

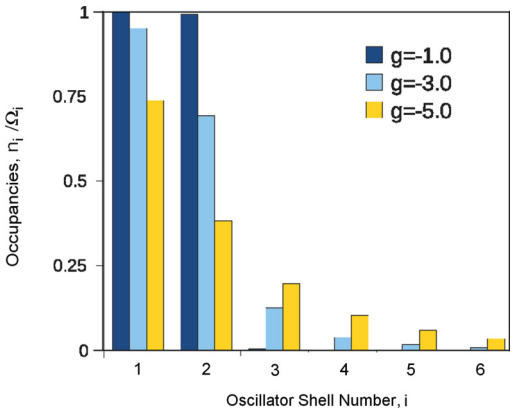


FIG. 17. (Color online) Occupancies (number of particles/degeneracy) of one-body states as a function of oscillator shell number for six particles at three interaction strengths for the ground state.

interesting to note that also the present pairing system can be described in terms of thermalization among the one-body states (Figs. 17 and 18), although we are dealing with a strongly coherent interaction, and chaos is suppressed. In fact, thermal melting of the Fermi surface proceeds faster than chaotization. The effective "temperature" is seen to increase with increasing pairing strength. For small to moderate pairing strength the thermalization is related to the initial steps of chaotic mixing. For higher strength, the temperature continues to increase, but the spectral properties suggest a regular many-body system. The appearance of an increasing thermalization as the system drives from mixed towards regularity, may be understood in the following way. If the wave functions of this regular state are expressed in the basis of the used basis, a very large number of components are needed, and, thus, the mixing or thermalization increases also when the system goes towards regularity. For example, the coherent states are indeed very mixed in the present basis.

On the other hand, the development of complexity with interaction strength looks quite similar for different particle numbers (see Fig. 6), suggesting that temperature is not a measure of complexity for the present system. As shown

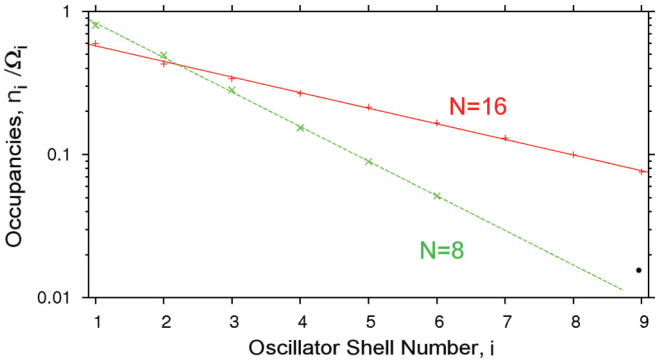


FIG. 18. (Color online) Occupancies (number of particles/degeneracy) of one-body states in logarithmic scale as a function of oscillator shell number for 8 particles (green crosses) and 16 particles (red plus signs). Pairing strength is $g = -5$. The straight lines are fits.

in Fig. 18, for a larger particle number the single-particle occupancies are falling much slower with increasing shell index, which can be considered as an indication of "higher temperature" in the larger system.

In general, this set of questions is related to the old problem of interrelation between the two languages of description for the excited states of a quantum system in a region of high level density. In a *mesoscopic system* we can use (i) the statistical description (temperature, thermal entropy, heat capacity, etc.) with averaging over the ensemble of states in a small energy window and (ii) the description using the individual stationary quantum states. The second approach in principle is more informative, especially if individual states can be prepared and studied experimentally. One can still argue that, under certain conditions, these approaches are not mutually exclusive but, rather, equivalent, with respect to certain type of questions. The mechanism of equivalence is provided by quantum many-body chaos. When the states become exceedingly complicated superpositions of many simple configurations, their wave functions (with the same exact quantum numbers) within that energy window "look the same" (ergodicity) [45]. The macroscopic observables then do not depend on the exact phase relationships between the wave-function components, and the description in terms of the thermal density matrix may be applied. In the present case we see, however, quite large differences between neighboring states (Fig. 9), and the ergodic hypothesis is not fulfilled.

## V. CONCLUSION

We have performed calculations on trapped fermionic atoms interacting with a short-ranged pairing-type force and examined the complexity of energies and wave functions for different particle numbers when the interaction strength is changed. Along with the appearance of pairing coherence in the ground and the first excited states, we have found a trend towards signatures of quantum chaos at intermediate interaction strength. The systematic chaotic behavior of more complicated systems, however, such as known in complex atoms and nuclei, is not reached. The pairing-type interaction applied in the present work, in addition to the generic selection rules valid for any two-body interaction, has other regular properties keeping intact conservation laws for partial seniorities and (two-dimensional) angular momentum. It is instructive that even such a regular interaction may lead to stochastic properties of the many-body system. If the coherent nature of the Hamiltonian is relaxed (as, for example, by using random signs of nondiagonal matrix elements), the system may become fully chaotic.

It is interesting to note that a system of contact-interacting atoms is the quantum analog of the gas of rigid spheres. This is one of the few many-body systems that have been strictly proven to be classically chaotic [46]. It was shown in Ref. [44] that, in the quantum gas of hard spheres, a random initial wave function evolves to a thermodynamical equilibrium momentum distribution corresponding to the specific statistics of the atoms, which is essentially quantum chaos. We have a very similar system but with attractive interactions. We found that in this case the road to chaos is long, at least in the case of

small particle numbers. Moreover, the path is reversed when the interaction is getting too strong and effectively leads to the regular degenerate pairing model. It would be interesting to go even further and see an analog of the BCS to BEC transition, where the chaotic features of the intermediate situation are usually not discussed.

For further work, systems that are more experimentally accessible should be examined. In addition to more realistic interactions, quantities such as the correlational entropy (see, for example, Ref. [47]) to look for possible phase transitions could be very interesting and testable experimentally.

## ACKNOWLEDGMENTS

S. Å. and S.M.R. thank the Swedish Research Council (VR) and the Nanometer Structure Consortium at Lund University for support. V.Z. acknowledges support through the NSF Grants No. PHY-0758099 and No. PHY-1068217.

[1] I. Bloch, J. Dalibard, and W. Zwerger, Rev. Mod. Phys. **80**, 885 (2008).
[2] F. Serwane, G. Zurn, T. Lomp, T. Ottenstein, A. Wenz, and S. Jochim, Science **332**, 6027 (2011).
[3] J. von Stecher, C. H. Greene, and D. Blume, Phys. Rev. A **77**, 043619 (2008).
[4] D. Blume, J. von Stecher, and C. H. Greene, Phys. Rev. Lett. **99**, 233201 (2007).
[5] J. von Stecher, C. H. Greene, and D. Blume, Phys. Rev. A **76**, 053613 (2007).
[6] M. Rontani, J. R. Armstrong, Y. Yu, S. Åberg, and S. M. Reimann, Phys. Rev. Lett. **102**, 060401 (2009).
[7] D. Blume, Rep. Prog. Phys. **75**, 046401 (2012).
[8] A. Bohr, B. Mottelson, and D. Pines, Phys. Rev. **110**, 936 (1958).
[9] S. T. Belyaev, Mat. Fys. Medd. K. Dan. Vidensk. Selsk. **31**, 11 (1959).
[10] A. Bohr and B. Mottelson, *Nuclear Structure*, Vol. 2 (Benjamin, New York, 1974).
[11] D. Brink and R. Broglia, *Nuclear Superfluidity: Pairing in Finite Systems* (Cambridge University Press, Cambridge, UK, 2005).
[12] A. Volya, B. A. Brown, and V. Zelevinsky, Phys. Lett. B **509**, 37 (2001).
[13] V. Zelevinsky and A. Volya, Phys. At. Nucl. **66**, 1781 (2003).
[14] V. V. Flambaum, A. A. Gribakina, G. F. Gribakin, and M. G. Kozlov, Phys. Rev. A **50**, 267 (1994).
[15] V. G. Zelevinsky, B. A. Brown, N. Frazier, and M. Horoi, Phys. Rep. **276**, 85 (1996).
[16] O. Bohigas, Nucl. Phys. A **751**, 343 (2005).
[17] S. Åberg, Phys. Rev. Lett. **64**, 3119 (1990).
[18] T. Guhr, Ann. Phys. **250**, 145 (1996).
[19] H. A. Weidenmüller and G. E. Mitchell, Rev. Mod. Phys. **81**, 539 (2009).
[20] D. M. Basko, I. L. Aleiner, and B. L. Altshuler, *Problems of Condensed-Matter Physics*, edited by A. L. Ivanov and S. G. Tikhodeev, Vol. 50 (Oxford University Press, Oxford, UK, 2008).
[21] T. A. Brody, J. Flores, J. B. French, P. A. Mello, A. Pandey, and S. S. M. Wong, Rev. Mod. Phys. **53**, 385 (1981).
[22] V. Zelevinsky, Ann. Rev. Phys. Nucl. Sci. **46**, 237 (1996).
[23] M. Matsuo, T. Døssing, E. Vigezzi, and S. Åberg, Nucl. Phys. A **620**, 296 (1997).
[24] M. Cambiaggio, A. Rivas, and M. Saraceno, Nucl. Phys. A **624**, 157 (1997).
[25] B. D. Esry and C. H. Greene, Phys. Rev. A **60**, 1451 (1999).
[26] A. Bulgac, J. E. Drut, and P. Magierski, Phys. Rev. Lett. **96**, 090404 (2006).
[27] I. Stetcu, B. R. Barrett, and U. V. Kolck, Phys. Lett. B **653**, 358 (2007).
[28] I. Stetcu, B. R. Barrett, U. van Kolck, and J. P. Vary, Phys. Rev. A **76**, 063613 (2007).
[29] Y. Alhassid, G. F. Bertsch, and L. Fang, Phys. Rev. Lett. **100**, 230401 (2008).
[30] M. Rontani, S. Åberg, and S. M. Reimann (2008). arXiv:0810.4305.
[31] J. R. Armstrong, M. Rontani, S. Åberg, V. G. Zelevinsky, and S. M. Reimann, Few-Body Syst. **45**, 219 (2009).
[32] B. French and S. S. M. Wong, Phys. Lett. B **33**, 449 (1970).
[33] D. R. Bes and R. A. Broglia, Nucl. Phys. **80**, 289 (1966).
[34] O. Bohigas, M. J. Giannoni, and C. Schmit, Phys. Rev. Lett. **52**, 1 (1984).
[35] T. A. Brody, Nuovo Cimento **7**, 482 (1973).
[36] F. M. Izrailev, Phys. Rep. **196**, 299 (1990).
[37] N. Frazier, B. A. Brown, and V. Zelevinsky, Phys. Rev. C **54**, 1665 (1996).
[38] C. Stoyanov and V. Zelevinsky, Phys. Rev. C **70**, 014302 (2004).
[39] V. V. Flambaum and F. M. Izrailev, Phys. Rev. E **61**, 2539 (2000).
[40] A. Volya, V. Zelevinsky, and B. A. Brown, Phys. Rev. C **65**, 054312 (2002).
[41] J. Dukelsky, J. Okołowicz, and M. Płoszajczak, J. Stat. Mech. (2009) L2007.
[42] V. V. Flambaum and F. M. Izrailev, Phys. Rev. E **56**, 5144 (1997).
[43] S. Åberg, Prog. Part. Nucl. Phys. **28**, 11 (1992).
[44] M. Srednicki, Phys. Rev. E **50**, 888 (1994).
[45] I. Percival, J. Phys. B **6**, L229 (1973).
[46] Y. G. Sinai, Russ. Math. Surv. **25**, 137 (1970).
[47] A. Volya and V. Zelevinsky, Phys. Lett. B **574**, 27 (2003).